

SAMPLING IN OPTICAL DIFFRACTION, RALEYGH-SOMMERFELD APPROACH

Juliana Pérez Hernández, Tomás Velez Acosta

^aUniversidad EAFIT, , Medellín, Colombia

Abstract

This paper presents an analysis of the proposed optimization approach aimed at reducing computational complexity and reconstruction time by reducing the hologram sampling in Lensless Holographic Microscopy (LHM). In contrast to other approaches, this study incorporates a nonlinear objective function and corresponding constraints based on the Nyquist criterion particularly in the spherical phase of the Raileygh Sommerfeld diffraction integral. The optimization method shows a huge potential allowing to save minutes (or more) time per reconstruction, addressing partially the reconstruction time problem and overcoming the limitations of traditional linear optimization techniques.

Keywords: Diffraction, Sampling, Nyquist Frequency, NLPP

1. Introduction

Lensless Holographic Microscopy (LHM) have demonstrated their ability to overcome the limitations of conventional lens systems in terms of portability and enhancing biological sampling (1; 2). However, one of the key challenges in these techniques lies in the computational complexity associated with image reconstruction, limiting their practical application in situations that require rapid image acquisition and efficient processing.

Reconstruction in LHM involves calculating the any numerical propagator. In particular, the Rayleigh Sommerfeld Diffraction integral (RS1) is a diffraction model that solves the scalar wave equation (i.e Helmholtz equation) and obtains reliable images in the reconstruction process (3). However, Its computational implementation is computationally intensive and may require long calculation times.

In recent years, there has been a growing interest in optimizing the computational complexity for lensless microscopy and the Rayleigh-Sommerfeld approximation. Researchers have explored various strategies, ranging from improving existing algorithms to implementing parallel approaches and hardware acceleration, with the aim of significantly reducing calculation time and enabling real-time acquisition and processing of microscopic images (4).

In this paper, we propose an alternative optimization framework that integrates a nonlinear objective function (the computational complexity) and incorporates the Nyquist criterion constraints for signal sampling. The aim is to improve the efficiency of image reconstruction by carefully finding the optimum sampling that minimizes the reconstruction time without suffering aliasing.

2. Problem Statement

Lensless Holographic Microscopy (LHM) is an optical optical technique that allows to retrieve information of amplitude

and phase of samples, usually biological samples. The set-up of a LHM is rather simple as shown below:

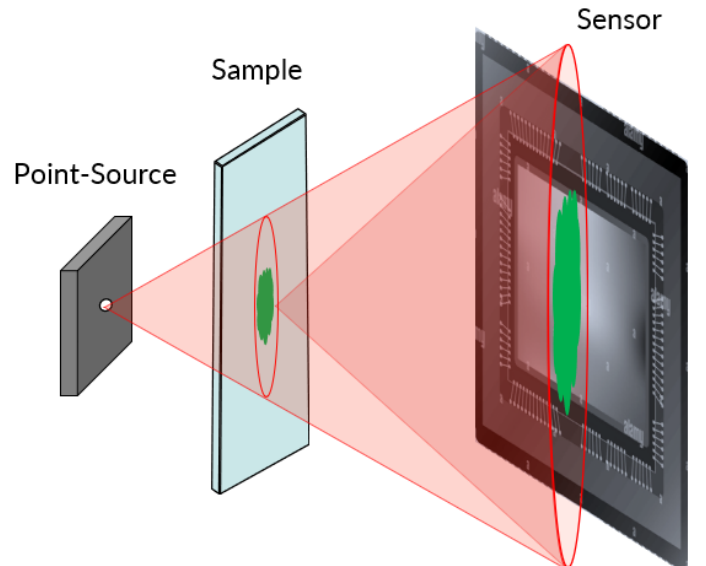


Figure 1: LHM Set-up

It essentially consists of a point-source and a camera. The spherical wavefront emitted by the point-source illuminates the sample producing a diffraction pattern which is then recorded by a digital sensor, usually a CCD or CMOS camera.

Since the system experimentally only allows the acquisition of a diffraction pattern, it is necessary a good model to reproduce (reconstruct in optical terms) the information of the sample. The theory behind the reconstruction process in holography is called Scalar Diffraction Theory. The model is deducted next in resemblance of the way it is deducted in (5).

2.1. Rayleigh-Sommerfeld Diffraction Integral

Consider the Maxwell laws of electromagnetism:

$$\begin{aligned}\nabla \cdot \mathbf{E} &= \frac{\rho}{\epsilon_0} \\ \nabla \cdot \mathbf{B} &= 0 \\ \nabla \times \mathbf{E} &= -\frac{\partial \mathbf{B}}{\partial t} \\ \nabla \times \mathbf{B} &= \mu_0 \mathbf{J} + \mu_0 \epsilon_0 \frac{\partial \mathbf{E}}{\partial t}\end{aligned}\quad (1)$$

When doing a proper analysis of the partial derivatives inside these equations, when can obtain two wave equations, one for the electric field, and one for the magnetic field:

$$\begin{aligned}\frac{1}{c_0^2} \frac{\partial^2 \mathbf{E}}{\partial t^2} - \nabla^2 \mathbf{E} &= 0 \\ \frac{1}{c_0^2} \frac{\partial^2 \mathbf{B}}{\partial t^2} - \nabla^2 \mathbf{B} &= 0\end{aligned}\quad (2)$$

Where $c_0 = \frac{1}{\sqrt{\mu_0 \epsilon_0}}$. One can see the magnitude of the energy stored in the electric field is orders of magnitude higher than the one in the magnetic field, hence, the analysis will be done to the first wave equation.

Taking just one component of this vectorial equation (namely, the x component) we get the expression:

$$\nabla^2 E_x - k^2 \frac{\partial^2 E_x}{\partial t^2} = 0 \quad (3)$$

which turns to be the Helmholtz equation:

$$\nabla^2 U + k^2 U = 0 \quad (4)$$

Now, centering this generalized expression into the boundary value problem that a is imposed by the necessity of knowing the field in a random plane parallel to bounding plane (the camera plane) where the field is known.

The way to obtain such a solution, relies on the integral Theorem of Helmholtz and Kirchhoff which ultimately states that the perturbation U at a given point P_0 can be calculated by the values of the perturbation at the boundary of a closed surface surrounding it as:

$$U(P_0) = \frac{1}{4\pi} \iint_S \left\{ \frac{\partial U}{\partial n} \left[\frac{\exp(jkr_{01})}{r_{01}} \right] - U \frac{\partial}{\partial n} \left[\frac{\exp(jkr_{01})}{r_{01}} \right] \right\} ds \quad (5)$$

Yet, this expression has yet to be modified to obtain a useful result. For instance, lets express the boundary conditions for this particular problem:

The closed surface composed by S_1 (The screen plane) and S_2 (The spherical hollow) allow us to use the Integral Theorem, yet, we only know the behaviour of the field in S_1 . Here is where we use the Sommerfeld radiation condition, which states that the perturbations we are trying to calculate, are at least spherically diverging perturbations, making the contributions of the field in S_2 negligible.

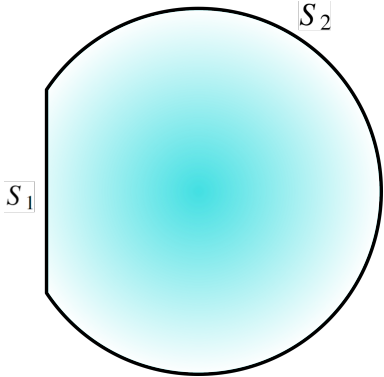


Figure 2: Boundary of the region to be solved

This results in dropping the integral over S_2 and resulting in the expression:

$$U(P_0) = \frac{1}{4\pi} \iint_{S_1} \left(\frac{\partial U}{\partial n} G - U \frac{\partial G}{\partial n} \right) ds \quad (6)$$

This is the general diffraction integral, and according to the Green function chosen, different diffraction formulae can be obtained. In particular, when choosing $G_-(P_1) = \frac{\exp(jkr_{01})}{r_{01}} - \frac{\exp(jk\vec{r}_{01})}{\vec{r}_{01}}$ the equation 6 is reduced to:

$$U_I(P_0) = \frac{-1}{4\pi} \iint_{\Sigma} U \frac{\partial G_-}{\partial n} ds. \quad (7)$$

Where Σ is the region of the camera in the input plane. This expression can also be written explicitly using the Green function above leading to:

$$U_I(P_0) = -\frac{1}{2\pi} \iint_{\Sigma} U(P_1) \left(jk - \frac{1}{r_{01}} \right) \frac{\exp(jkr_{01})}{r_{01}} \cos(\vec{n}, \vec{r}_{01}) ds \quad (8)$$

The expression 8 is known as the Rayleigh Sommerfeld Diffraction integral (shortly RS1) and is the expression one of the authors is proposing as an alternative to reconstruct the diffraction patterns in LHM (after different authors (3) reviewed its feasibility and good experimental results).

2.2. Discretization

To be used computationally, this expression clearly needs to be discretized since the sensors used to store the diffraction patterns are also discretized in an array of pixels. The discrete expression is then written as:

$$\begin{aligned}U(p\Delta x, q\Delta y, z) &= -\frac{1}{2\pi} \sum_{m=1}^M \sum_{n=1}^N U(m\Delta x_0, n\Delta y_0, 0) \left(jk + \frac{1}{r} \right) \\ &\times \frac{\exp(jkr)}{r} \frac{z}{r} \Delta x_0 \Delta y_0,\end{aligned}\quad (9)$$

with $r = \sqrt{(p\Delta x - m\Delta x_0)^2 + (q\Delta y - n\Delta y_0)^2 + z^2}$ (3). From this expression it follows that if for x and y we have m, μ and n, η number of pixels, computationally this method would have a complexity of $O(m \cdot \mu \cdot n \cdot \eta)$ which is in general terms high,

at least not practical for its usage in LHM (the focusing problem makes it necessary to have at least 10 reconstruction per hologram to find the sample plane). Nonetheless, this model was implemented and using few pixels, it was noticeable that sampling is crucial to allow a proper reconstruction. In figure 3 different sampling was used with the same physical reconstruction parameter, and it is clear that aliasing is a problem knowing that we want to use the least amount of pixels possible to achieve the best reconstruction time without compromising the quality of the results. The conclusion to which we arrived is that Nyquist Shannon Theorem as presented in (6) is a restriction that must be satisfied.

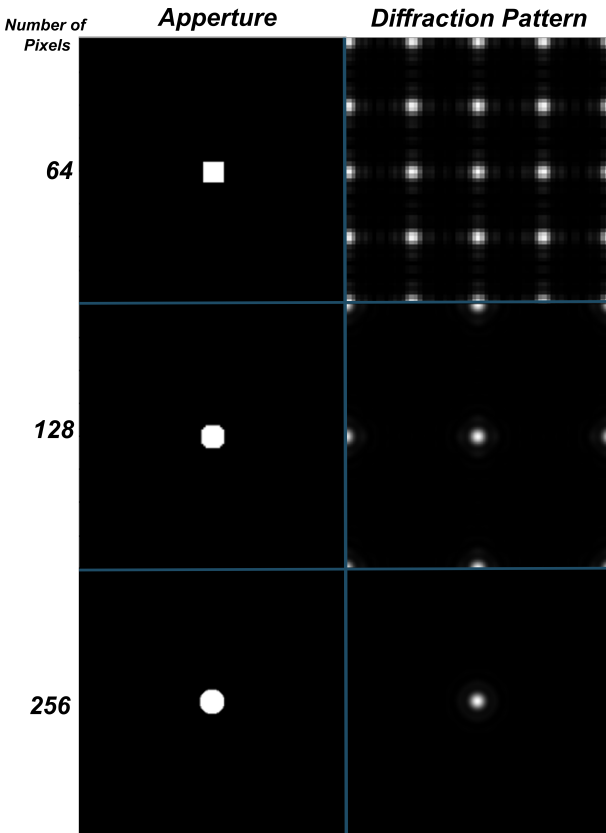


Figure 3: Aliasing due to bad sampling

2.3. Optimization problem

In all this context, the authors of this paper reached a proposal to optimize the computational complexity of the algorithm in terms of the number of pixels in the reconstruction of the hologram (μ, η) using as restriction the Nyquist-Shannon theorem on each axis. Hence, the problem shall be expressed as the next Non Linear Programming Problem:

$$\begin{aligned} & \min O = m \cdot n \cdot \mu \cdot \eta \\ \text{r.t. } & \mu \geq \frac{2dx_{in}^2(M+M^2)}{\lambda} \frac{m^2}{\sqrt{z^2+dx_{in}^2(1+M)^2m}} \\ & \eta \geq \frac{2dy_{in}^2(M+M^2)}{\lambda} \frac{n^2}{\sqrt{z^2+dy_{in}^2(1+M)^2n}} \end{aligned} \quad (10)$$

In the problem presented in equation 10, (m, n) are the dimensions of the input plane in pixels, (dx_{in}, dy_{in}) are the pixel

pitches of the input plane (experimentally they are given by the sensor pitch), M is the magnification in the propagation, a relationship between the physical sizes of the output and input planes ($M = \frac{W_{out}}{W_{in}}$), z is the propagation distance and λ is the wavelength of the light to be propagated.

The restrictions are a modified form of the Nyquist theorem as presented in (6), taking into account the Magnification factor to condense the widths of the input and output planes, and the output pixel pitch.

3. Methodology

To successfully carry out the project, a methodology based on a to-do list was employed to follow a regular pipeline that leads to the desired outcome, despite encountering difficulties or abrupt changes in the development of the problem at hand.

3.1. SCRUM Methodology

Scrum is an agile project management methodology aimed at delivering high-quality products efficiently. It is based on principles of iterative and incremental development, emphasizing flexibility, collaboration, and continuous improvement. Scrum divides the project into short iterations called "sprints," typically lasting from one to four weeks, during which a prioritized set of work is completed.

The implementation of the Scrum methodology involves the following key elements:

- **Scrum Team:** A Scrum team is composed of three main roles: the Product Owner, the Scrum Master, and the Development Team. The Product Owner is responsible for defining and prioritizing product elements, representing the customer's interests and ensuring the product's value. The Scrum Master is the process facilitator, ensuring that Scrum practices are followed and removing obstacles that may affect the team. The Development Team is responsible for carrying out the work and delivering product increments.
- **Product Backlog:** The Product Owner is responsible for maintaining and managing the Product Backlog, which is a prioritized list of all functionalities, improvements, and requirements to be addressed in the project. The Product Backlog is flexible and can evolve as more information is obtained and requirements change.
- **Sprint Planning:** At the beginning of each sprint, the Scrum team holds a sprint planning meeting. During this meeting, the Product Owner presents the items from the Product Backlog that will be addressed in the sprint, and the Scrum team defines how the work will be carried out and delivered. The team selects items from the Product Backlog and breaks them down into smaller tasks.
- **Sprint:** During the sprint, the Scrum team works on completing the tasks defined in the sprint planning. The team has autonomy to organize and carry out their work. Daily

Scrum meetings are held to review progress and identify potential obstacles. The team strives to complete the planned work for the sprint.

- Sprint Review: At the end of each sprint, a sprint review meeting is held where the Scrum team showcases the completed product increments from the sprint. Feedback is obtained from the Product Owner and other stakeholders, and the achievement of the sprint goal is evaluated.
- Sprint Retrospective: After the sprint review meeting, the Scrum team conducts a sprint retrospective. In this meeting, the team reflects on the previous sprint, identifies what worked well and what can be improved, and defines concrete actions to implement improvements in the next sprint.
- Iteration of Sprints: The process is repeated in successive iterations, with the Scrum team working on consecutive sprints to develop the product incrementally. As the project progresses, product increments are delivered until the final goal is achieved.

The Scrum methodology is characterized by its collaborative, adaptive, and transparent approach.

3.2. Kanban Methodology

The Kanban methodology is a visual management approach used to optimize workflow and improve efficiency in processes. It is based on the principle that work is divided into different stages and visualized through Kanban boards. The implementation of the Kanban methodology involves the following steps:

- Identify the workflow: It starts by understanding and mapping the existing workflow. This involves identifying the different stages or activities involved in the process, from the initial request to the completion of work.
- Define Kanban board columns: Each stage of the workflow is represented as a column on the Kanban board. For example, columns can be "To Do," "In Progress," and "Completed." Additional columns can be added based on specific process needs.
- Create Kanban cards: Each work or task is represented by a Kanban card. These cards contain relevant information such as task description, responsible person, and any associated deadlines.
- Establish Work in Progress (WIP) limits: To avoid overload and optimize workflow, maximum limits are set for the number of Kanban cards allowed in each column. This helps maintain a balanced flow of work and prevents bottlenecks.
- Visualize and move Kanban cards: Kanban cards are initially placed in the "To Do" column. As progress is made in the process, cards are moved to the corresponding column. This provides a clear visualization of the status of each task and helps identify potential delays or issues.

- Follow the "Pull" principle: Instead of assigning tasks, team members pull Kanban cards from the "To Do" column based on their capacity and availability. This ensures a balanced workflow and avoids the accumulation of tasks in the hands of a single team member.
- Continuously review and improve: The Kanban methodology promotes a continuous improvement approach. As it is implemented and used, areas for improvement can be identified, and adjustments can be made to the workflow, WIP limits, and other aspects to further optimize the process.

4. Results and Discussion

The implemented algorithm to solve this NLPP uses the SLSQP method since the target function is quadratic, and it is presented in the flowchart of figure 4.

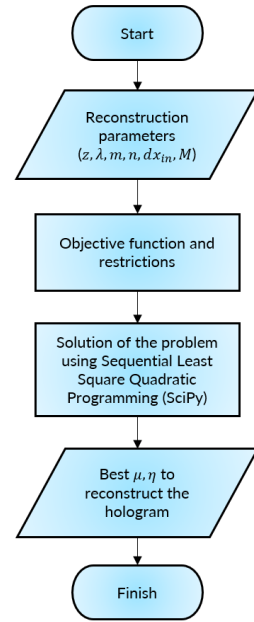


Figure 4: Flowchart describing the algorithm that solves the proposed problem

The code was implemented in Python and can be accessed easily through the Colab Notebook [Sampling Optimization](#) (bit.ly/sampling_optimization).

Using the solutions to the problem given by the algorithm, the RS1 was tested purposely under and sharply on the solution to see whether this sampling effectively got rid off the aliasing. The results are presented in figure 5, where instead of using the intensity of the diffracted field, we used the phase since it is more sensitive to any sampling operations. Notice that for the purposely aliased image, in the red circle, there is a new pattern that resembles the center of an spherical phase map, yet, after sampling the same geometry under the optimizer solution, this patterns disappeared, allowing to construct the image in just 239 s contrary to the typical powers of two criteria here it would have required 512 pixels requiring around one hour of calculations.

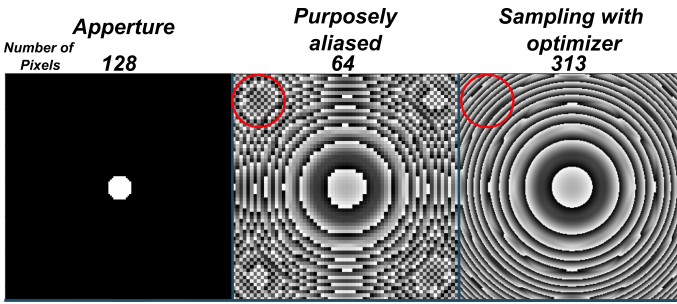


Figure 5: Comparison of the diffracted phase map with aliasing and without aliasing (using the sampling that the optimizer found).

5. Summary and conclusions

The implementation of an optimization model to properly sample the output in a computationally heavy diffraction model such as the Rayleigh-Sommerfeld diffraction Integral allows the reconstruction process to operate with the best time possible without compromising the reconstruction with aliasing. Besides, the fact that the implementation was made in python directly allows the next step which would be including this calculation inside the code of the RS1, making it self sufficient in the selection of the output sampling. This result accompanied with currently developing implementation of the RS1 using parallel programming in GPU can make this reconstruction technique more competitive against the traditional methods in terms of computation time.

Acknowledgements

Thanks to Ph.D Carlos Trujillo and Ph.D Christian Montoya for their advise in the optical and mathematical aspects of this research, the School of Applied Sciences and Engineering for the opening of the course Optimization 1, and in general EAFIT University for its support in terms of equipment and infrastructure required for the proper development of the course and particularly this project.

References

- [1] W. Xu, M. H. Jericho, I. A. Meinertzhangen, and H. J. Kreuzer, "Digital in-line holography for biological applications," *Proceedings of the National Academy of Sciences of the United States of America*, vol. 98, no. 20, pp. 11301–11305, 2001.
- [2] M. J. Lopera and C. Trujillo, "Linear diattenuation imaging of biological samples with digital lensless holographic microscopy," *Applied Optics*, vol. 61, no. 5, p. B77, 2022.
- [3] C. Buitrago-Duque and J. Garcia-Sucerquia, "Non-approximated Rayleigh–Sommerfeld diffraction integral: advantages and disadvantages in the propagation of complex wave fields," *Applied Optics*, vol. 58, no. 34, p. G11, 2019.
- [4] P. Piedrahita-Quintero, C. Trujillo, and J. Garcia-Sucerquia, "JDiffract: A GPGPU-accelerated JAVA library for numerical propagation of scalar wave fields," *Computer Physics Communications*, vol. 214, pp. 128–139, 2017.
- [5] J. Goodman, *Introduction to Fourier Optics*. McGraw-Hill, second ed., 1996.
- [6] S. Mehrabkhani and T. Schneider, "Is the Rayleigh-Sommerfeld diffraction always an exact reference for high speed diffraction algorithms?," *Optics Express*, vol. 25, no. 24, p. 30229, 2017.
- [7] H. Lichte, "Electron holography approaching atomic resolution," *Ultramicroscopy*, vol. 20, no. 3, pp. 293–304, 1986.
- [8] H. J. Kreuzer, K. Nakamura, A. Wierzbicki, H. W. Fink, and H. Schmid, "Theory of the point source electron microscope," *Ultramicroscopy*, vol. 45, no. 3-4, pp. 381–403, 1992.
- [9] J. Garcia-sucerquia, W. Xu, S. K. Jericho, P. Klages, M. H. Jericho, and H. J. Kreuzer, "Digital in-line holographic microscopy," 2006.
- [10] H. J. Kreuzer, "HOLOGRAPHIC MICROSCOPE AND METHOD OF HOLOGRAM RECONSTRUCTION," 2002.
- [11] P. Piedrahita-Quintero, R. Castañeda, and J. Garcia-Sucerquia, "Numerical wave propagation in ImageJ," *Applied Optics*, vol. 54, no. 21, p. 6410, 2015.
- [12] M. K. Kim, "Principles and techniques of digital holographic microscopy," *SPIE Reviews*, vol. 1, no. 1, 2010.
- [13] D. Gabor, "A new microscopic principle," *Nature*, vol. 161, no. 4098, pp. 777–778, 1948.